Open Access Journal

Journal of Sustainable Research in Engineering 1 (2) 2014, 34-39

Journal homepage: www.jkuat-sri.com/ojs/index.php/sri/index

Simulation of Saturation Efficiency and Cooling Capacity of an Unloaded Near Infrared Reflecting Charcoal Cooler for On-farm Storage of Mango fruits

Meshack K. Korir[1*], Urbanus Mutwiwa[1], Gareth M. Kituu[1] and Daniel N. Sila[2]

[1]*Department of Biomechanical and Environmental Engineering, Jomo Kenyatta University of Agriculture and Technology P.O BOX 62000-00200, Nairobi, Kenya*

[2]*Department of Food Science and Technology, Jomo Kenyatta University of Agriculture and Technology P.O BOX 62000-00200, Nairobi, Kenya*

[*]*Corresponding Author - E-mail: meshkorir2005@yahoo.com*

Abstract Mango (*Mangifera indica L.*) fruit is a valuable fruit in Kenya due to its nutritive value and economic importance. However, at least 40 to 45% of mango fruit is lost during postharvest handling primarily due to inadequate storage facilities for mango fruits. In this study, saturation efficiency and cooling capacity of an unloaded improved evaporatively cooled store for on-farm storage of mango fruits were simulated. The cooler had a storage space of 0.75 m^3 and its dimensions were 0.84 m x 0.84 m x 1.5 m. The external surfaces of the cooler were sprayed with a near infrared reflecting (NIR) paint. The cooler was constructed from locally available materials including hardwood and charcoal. The charcoal was kept moist by water dripping by gravity from horizontally laid pipes on the roof. The flow of water from an overhead tank approximately 2 m high to the cooler was monitored using a flow meter. The excess water which dripped was collected by gutters fixed at the lower ends of the charcoal walls and channeled to a water reservoir. A 12V pump was used to pump the water back to the overhead tank while a 12V fan located centrally on one of the sides directly opposite the door was used to draw air into the cooler. The pump and fan was powered by a 70Ah battery recharged by a 125 W solar panel. A computer model to simulate the saturation efficiency and cooling capacity of the cooler was developed on a java platform. The input parameters of the model were inlet air conditions, water conditions, air properties at selected ambient condition, and charcoal cooler characteristics. At varied inlet air velocities ranging from 3.0 m/s to 4.0 m/s at an interval of 0.2 m/s, the actual saturation efficiency of the cooler ranged from 68.9% to 66.9% while the predicted ranged from 69.0% to 66.9%. The actual cooling capacity of the cooler ranged from 1055667 kJ/h to 136477 kJ/h while the predicted ranged from105726 kW/h to 136680 kW/h. The high coefficient of determination (R^2=0.999) indicated a strong correlation between the actual and predicted results. A root mean square error (RMSE) corresponding to the actual and predicted saturated efficiency was 0.028% while that corresponding to the actual and predicted cooling capacity was 118 kJ/h. At 95% level of confidence, t test results showed no significant difference ($t_{calculated}$, 0.06; $t_{critical,}$ 2.23) between the actual and predicted saturation efficiency. The t test results also indicated no significant difference ($t_{calculated,}$ 0.01; $t_{critical,}$ 2.23) between the actual and predicted cooling capacity.

Keywords Cooling capacity, mango fruit, near infrared reflecting (NIR) charcoal cooler, saturation efficiency, simulation model

1 Introduction

Mango (*Mangifera indica L.*) is an adaptable fruit tree in Kenya, suitable for different agro-ecological zones ranging from sub-humid to semi-arid [1]. Mango tree thrives well at 0 to 1500 m above sea level in Kenya although it can grow in higher elevations [2]. In Kenya, an output of 280,884 metric tonnes of mango fruit is produced at an estimated production area of 14,387 Ha [3]. Coast and the semi-arid counties of Eastern Kenya are the main production areas of mangoes.

Mango fruit is known for its nutritive value and economic importance. It is a potential source of income for resource poor farmer. It is also a source of raw material for industries and foreign exchange earner. However, mango fruits are riddled with challenges along the post-harvest chain. At least 40 to 45% of the fruit is lost along the post-harvest chain [4]. Mechanical damage (bruises), pests and diseases and immature harvesting are the causes of losses. Postharvest losses are also due to inadequate storage facilities for mango fruits during peak harvesting periods.

It is possible to develop effective storage systems and use them to reduce the losses thus improving the net returns for the resource poor farmers [5]. An effective storage of mango fruits can be achieved by controlling the storage environment. The critical parameters in the modern storage systems include; temperature, moisture and humidity, air velocity, lighting, odour, and pressure [6, 7]. During storage, it is important to ensure mango fruits stored are of good quality and free from damages or diseases. The damaged or diseased fruits respire rapidly and consequently produce more heat. In addition, the fruits are exposed to microbial attack [8]. In this study, a computer model was developed to simulate saturation efficiency and cooling capacity of an improved evaporatively cooled store for on-farm storage of mango fruits. This paper presents the model results of an unloaded near infrared reflecting (NIR) charcoal cooler.

2 Methodology

2.1 Development of a near infrared charcoal cooler

An improved charcoal cooler suitable for preservation of mango fruits was developed and its performance tested in the Department of Biomechanical and Environmental Engineering, Jomo Kenyatta University of Agriculture and Technology (JKUAT). The cooler was constructed from locally available materials including hardwood timber (10 cm x 5 cm), hardwood strips (5 cm x 2.5 cm), charcoal, welded wire mesh of wire diameter of 0.24 mm and wire spacing of 7.5 cm, coffee tray mesh of wire diameter of 0.5 mm and wire spacing of 5 mm), and aluminium sheet of gauge 24 and thickness of 0.5 mm.

The external surfaces of the cooler were sprayed with near infrared reflecting (NIR) paint (redusol). The cooler had a storage space of 0.75 m^3 and its dimensions were 0.84 m x 0.84 m x 1.5 m. The cooler had two walls and a doom-shaped aluminium roof filled with 10 cm charcoal layer. The charcoal was held firmly by coffee tray mesh reinforced with the welded mesh. The charcoal was kept moist by water dripping by gravity from a horizontally laid 12.7 mm polypropylene random copolymers (PPR) pipes on the roof. The excess water was collected by gutters fixed at the lower ends of the charcoal walls and channeled to a water reservoir. A 12V shurflo pump with a capacity of 13.2 l/min and 2.7 m head (model 2088-443-144, Mexico) was used to pump water from the reservoir back to an overhead tank approximately 2 m from the ground.

The amount of water used to moisten the charcoal was monitored using a 12.7 mm multi-jet vane wheel dry type water flow meter. The air was drawn into the cooler by a 12V fan centrally located on one of the sides directly opposite the door. A 70Ah battery which was re-charged by a 125 W solar panel was the main power source for the fan and pump. A charge controller (model Apple 15, Sundaya international, Singapore) was used to control the battery from overcharging.

2.2 Development of a computer simulation model

A computer model to simulate saturation efficiency and cooling capacity of the cooler was developed on a java platform. The inputs parameters of the model were inlet air condition: dry bulb temperature (^oC), wet bulb temperature (^oC), specific humidity (kg/kg of dry air), and velocity (m/s); water condition: water temperature (^oC), and water flow rate (l/s); charcoal cooler characteristics: length of the evaporative pad (m), evaporative pad thickness (m), height of the evaporative pad (m), and wetted area per unit volume of charcoal material (m^2/m^3), air properties: specific heat of air (J/kgK), specific heat of the water vapor (J/kgK), thermal conductivity of air (W/mK), Prandtl number (dimensionless), kinematic viscosity of air (m^2/sec), and density of air (kg/m^3).

The output parameters of the model included: total face area of the evaporative pads (m^2), total face area through which the air enters the evaporative pad (m^2), total wetted surface area of the evaporative pad (m^2), characteristic dimension (m), Nusselt number (dimensionless), Reynolds number (dimensionless), air mass flow rate (kg/s), convective heat transfer coefficient of air (W/m^2K), saturation efficiency (%), specific heat of humid air (J/kgK), dry bulb temperature of the outlet air (^oC), and cooling capacity (kW/h). The dry bulb temperature and relative humidity of the inlet air were measured on hourly basis while the wet bulb temperature and specific humidity of the inlet air was computed using psychrometric calculator. The air properties were evaluated at the selected ambient condition.

2.3 Ambient condition

Daily dry bulb temperature (T_{db}) and relative humidity (RH) data of Jomo Kenyatta University of Agriculture and Technology (JKUAT), Juja, Kenya (latitude, -1.1^o; longitude, 37.02^o; altitude, 1211m above the sea level) for the month of January, February and March, 2014 were collected and grouped into 5 categories (Table I).

Table 1: Weather data of the Jomo Kenyatta University of Agriculture and Technology, Juja, for the month of January, February, and March, 2014

Ambient condition	Maximum, T_{db} (°C)	Total days	Mean Maximum, T_{db} (°C)	Mean RH (%)	Mean T_{wb} (°C)
A	Below 25.5	3	24.1	80.6	21.5
B	25.6 to 27.5	9	26.4	76.4	23.2
C	27.6 to 29.5	23	28.7	66.8	23.9
D	29.6 to 31.5	35	30.5	60	24.4
E	Above 31.6	20	32.2	52.4	24.6

The most occurring ambient condition D (Table 1) of mean maximum T_{db} of 30.5°C and RH of 60% were selected for analysis. All the air properties were evaluated based on this condition that is the specific heat of air was 1005 J/kgK, specific heat of water vapor, 1865 J/kgK, thermal conductivity of air, 0.02644 W/mK, Prandt number, 0.7135, kinematic viscosity of air, 16.09×10^{-6} m^2/s, and density of air was 1.164 kg/m^3.

2.4 Geometrical dimensions of the evaporative pad and set up

Fig. 1 shows geometrical dimensions of the evaporative pad. Fig. 2 indicates the direction of air flow in the cooler and arrangement of the evaporative pads. A 12V fan drew the ambient air from one of the sides of the charcoal cooler directly opposite the door. The air was then channeled through 25 mm spacing between aluminium sheet and the charcoal wall (Fig.2). The lateral sections of the walls were completely closed and hence the air exited on the open side of the wall.

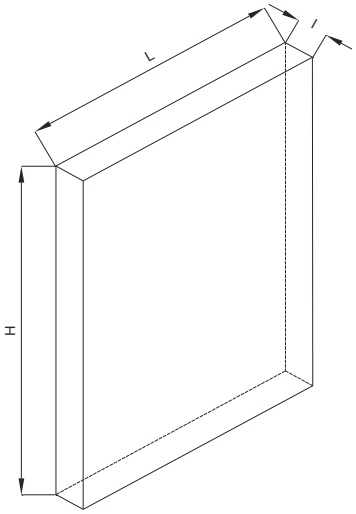

Fig. 1. Geometrical dimensions of the evaporative pad

2.5 Mathematical modelling

The area through which air enters the pad was taken as face area. The total face area of the two pads was determined based on equation 1. In this equation, L is the length of the pad 0.84 m; H is the height of the pad, 1.1 m, and A_{ft} is the total face area through which air enters the pad, 1.848 m^2.

$$A_{ft} = 2(L \times H) \quad (1)$$

The total volume of the pads is given by equation 2. I is the thickness of the pad, 0.1 m, and ϑ is the total volume of the pads, 0.1848 m^3.

$$\vartheta = 2(L \times H \times I) \quad (2)$$

Total wetted surface area for the charcoal pads was determined using equation 3. A_v is wetted area per unit volume of charcoal material, 500 m^2/m^3; and A_w is total wetted area of the evaporative pads, 92.4 m^2.

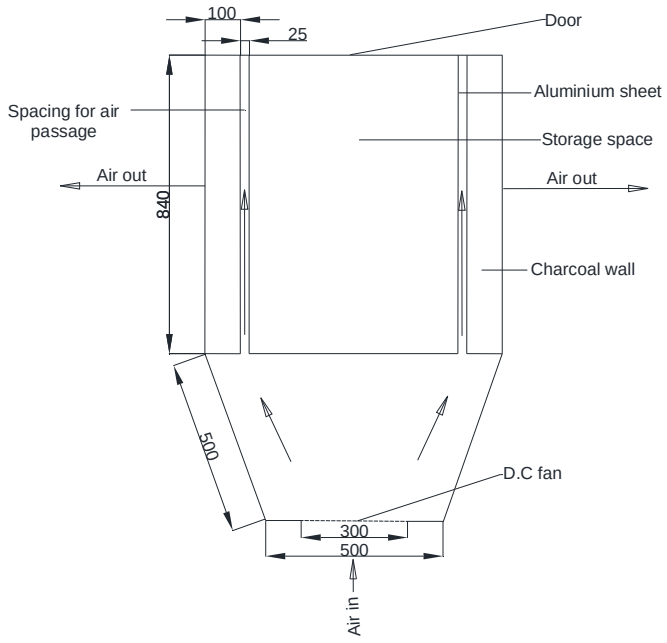

Fig. 2. A top view of the near infrared reflecting (NIR) charcoal cooler showing the direction of air flow arrangement of evaporative pads. All the dimensions are in mm.

$$A_w = \vartheta \times A_v \quad (3)$$

Characteristic dimension was given by equation 4. l_c is the characteristics dimension, 0.002 m.

$$l_c = \frac{\vartheta}{A_w} \quad (4)$$

Convective heat transfer coefficient was determined based on equation 5 [9]. In this equation, Nu is the Nusselt number (dimensionless), Re is the Reynolds number (dimensionless), and Pr is the Prandtl number (dimensionless).

$$Nu = 0.10\left[\frac{l_c}{l}\right]^{0.12} \mathrm{Re}^{0.8}\ \mathrm{Pr}^{0.33} \quad (5)$$

Reynolds number was given by equation 6 [10]. v_a is the air velocity of air through the charcoal pad (m/s), and v is the kinematic viscosity of air.

$$\mathrm{Re} = \frac{v_a l_c}{v} \quad (6)$$

Predicted saturation efficiency was computed using equation 7 [9]. η_p is the percentage predicted saturation efficiency, h_c is the convective heat transfer coefficient (W/m^2K), m_a is the mass flow rate of air through the pad (kg/s), and c_{pu} is the specific heat of humid air (J/kgK).

$$\eta_p = \left[1 - \exp\left(-\frac{h_c A_w}{m_a c_{pu}}\right)\right] * 100 \quad (7)$$

Convective heat transfer coefficient of air was computed using equation 8. h_c is the convective heat transfer coefficient of air (W/m^2K) and K_a is the thermal conductivity of air (W/mK).

$$h_c = \frac{Nu \times k_a}{l_c} \quad (8)$$

Specific heat of humid air was given by equation 9. c_{pu} is the specific heat of water vapor, c_{pa} is the specific heat of air (J/kgK), c_{pv} is specific heat of the water vapor (J/kgK), and w is the specific humidity (kg/kg of dry air).

$$c_{pu} = c_{pa} + wc_{pv} \quad (9)$$

Mass flow rate of air was determined using equation 10. Ma is the mass flow rate of air (kg/s) and ρ is the air density (kg/m^3).

$$m_a = A_{ft} \times v_a \times \rho \quad (10)$$

The predicted dry bulb temperature of outlet air was calculated using equation 11 [10]. t_1 is actual dry bulb temperature of the inlet air (°C), t_p is predicted dry bulb temperature of the outlet air (°C), t_{wbt} is wet bulb temperature of the inlet air (°C).

$$t_p = t_1 - 0.01\eta(t_1 - t_{wbt}) \quad (11)$$

The predicted cooling capacity of the cooler was evaluated based on equation 12 [10]. Q_p is the predicted cooling capacity (kJ/h).

$$Q_p = m_a c_{pa}(t_1 - t_p) * 3.6 \quad (12)$$

2.6 Data acquisition

Dry bulb temperature and relative humidity of the inlet and outlet air were measured on hourly basis during the testing period of the cooler from 8a.m to 6p.m. using Tinytag Ultra 2 data logger (model TGU-4500, Gemini Data Loggers Limited, United Kingdom). The inlet air velocity was measured using EMPEX digital electronic anemometer wind Messe (model FG-561, Japan). A slide rheostat (Type, D-4; Amps, 8; Ohms, 2.8; No, Y-95; Yambishi Electric Co. Tokyo Japan) connected in series with the fan was used to vary inlet air velocities from 3.0 m/s to 4.0 m/s at an interval of 0.2 m/s. The saturation efficiency and cooling capacity of the cooler was simulated at these velocities.

The actual saturation efficiency was calculated using equation 13. In this equation, η_a is the percentage actual saturation efficiency, t_{wbt} is the wet bulb temperature of the inlet air computed using psychrometric calculator, t_1 and t_a is the actual inlet and outlet air dry bulb temperature, respectively.

$$\eta_a = \left(\frac{t_1 - t_a}{t_1 - t_{wbt}}\right) \times 100 \quad (13)$$

The actual cooling capacity of the cooler was calculated based on equation 14. Q_a is the actual cooling capacity (kJ/h).

$$Q_a = m_a c_{pa}(t_1 - t_a) * 3.6 \quad (14)$$

3 Results and discussion

Table 2 shows the output parameters of the model when

the cooler was evaluated at varied inlet air velocities at no load condition (Fig.3).

Table 2: Output parameters of the model at varied inlet air velocities

Parameter	Value					
V_a (m/s)	3.0	3.2	3.4	3.6	3.8	4.0
Nu (dimensionless)	6.4	6.7	7.0	7.4	7.7	8.0
Re (dimensionless)	373	398	423	447	472	497
ma (kg/s)	6.5	6.9	7.3	7.7	8.2	8.6
h_c (W/m^{2}K)	84.3	88.8	93.2	97.5	101.8	106.1
η_o (%)	69.0	68.5	68.1	67.6	67.2	66.9
c_{pa} (J/kgK)	1031.3	1031.4	1031.3	1031.3	1031.3	1031.3
t_p (°C)	24.54	24.56	24.6	24.62	24.65	24.67
Q_o (kJ/h)	105726	110804	118241	124429	130575	136680

The saturation efficiency of the cooler at varied inlet air velocities ranged from 69.0% to 66.9% while the cooling capacity ranged from 105726 kJ/h to 136680 kJ/h (Table 2). The actual saturation efficiency ranged from 68.9% to 66.9% while the cooling capacity ranged from 105667 kJ/h to 136477 kJ/h (Table 3). The saturation efficiency and cooling capacity varies with inlet air velocity. The saturation efficiency decreases with increase in the inlet air velocity. At higher velocities, air has lesser contact time with water causing less evaporation [10]. Fig. 4 shows variation in saturation efficiency with inlet air velocity. The dry bulb temperature of the outlet air increases with decrease in saturation efficiency. The dry bulb temperature of the outlet air is directly affected by the saturation efficiency [10].

Fig. 3. An unloaded near infrared reflecting (NIR) charcoal cooler

The cooling capacity increases with increase in air velocity (Fig. 5). This implies large mass of air can be cooled at high inlet air velocity but at low saturation efficiency. The high coefficient of determination (R^2=0.999) indicated a strong correlation between the actual and predicted results. Thus, the model is more reliable for predicting the performance of the near infrared reflecting charcoal cooler. The root mean square error (RMSE) corresponding to actual and predicted saturation efficiency was 0.028% while that corresponding to actual and predicted cooling capacity was 118 kJ/h. T test results corresponding to the predicted and actual saturation efficiency indicated no significant difference ($t_{calculated}$, 0.06; $t_{critical}$, 2.23) at 95% level of confidence. T test results also showed no significant difference ($t_{calculated}$, 0.01; $t_{critical}$, 2.23) between the predicted and actual cooling capacity.

Table 3: Actual performance parameters of NIR charcoal evaluated at various inlet air velocities

Inlet air velocity (m/s)	η_a (%)	Q_a (kJ/h)
3.0	68.9	105667
3.2	68.5	111945
3.4	68.0	118134
3.6	67.6	124289
3.8	67.2	130489
4.0	66.9	136477

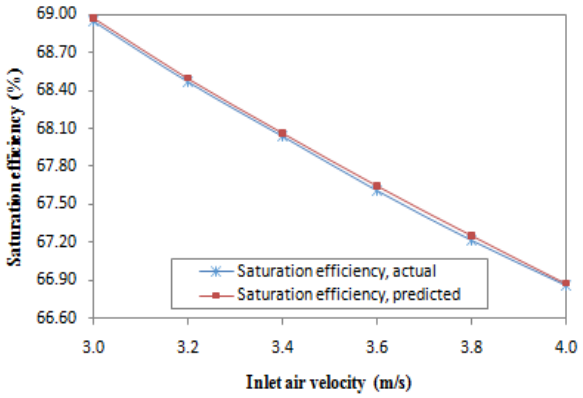

Fig. 4. The actual and predicted saturation efficiency of the near infrared reflecting (NIR) charcoal cooler

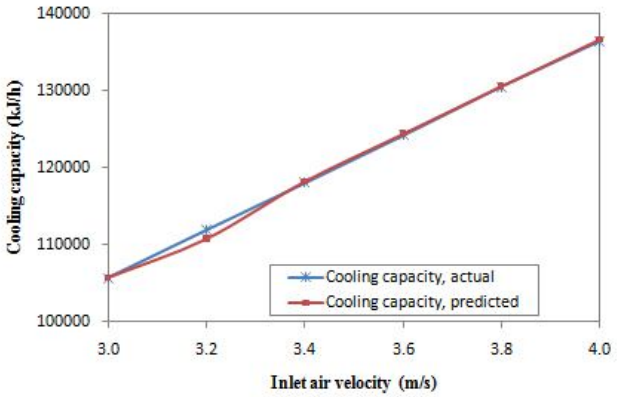

Fig. 5 The actual and predicted cooling capacity of the near infrared reflecting (NIR) charcoal cooler

Fig. 6 shows a computer model for simulating the saturation efficiency and cooling capacity of a NIR charcoal cooler.

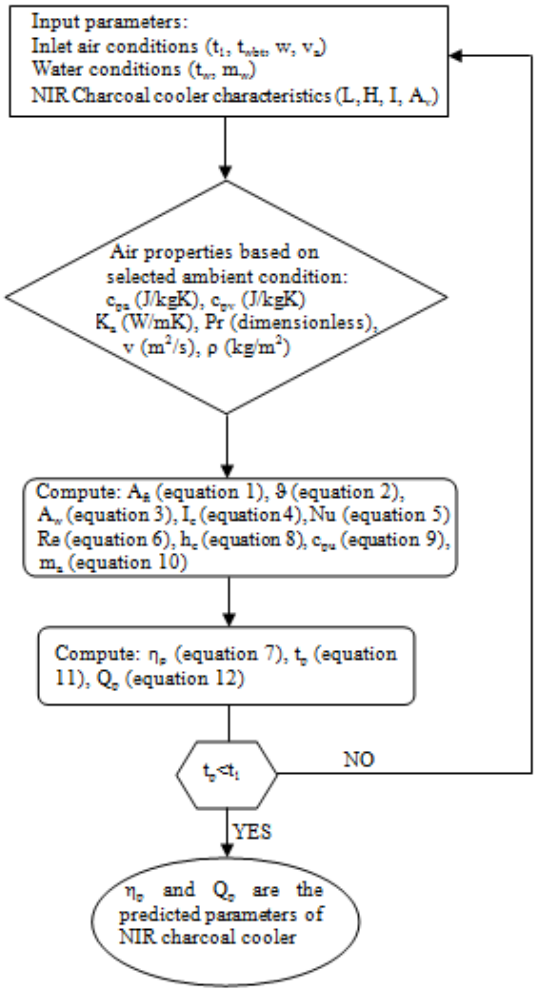

Fig. 6. A schematic computer model for simulating saturation efficiency and cooling capacity of the near infrared reflecting (NIR) charcoal cooler

4 Conclusions

The predicted saturation efficiency of the cooler ranged from 69.0% to 66.9% while the actual ranged from 68.9% to 66.9%. The predicted cooling capacity ranged from 105726 kJ/h to136680 kJ/h while the actual ranged from 105667 kJ/h to 136477 kJ/h. T test results indicated no significant difference between the actual and predicted results. The high coefficient of determination and low root mean square error (RMSE) obtained showed high reliability of the model.

Acknowledgements

The authors would like to thank the Jomo Kenyatta University of Agriculture and Technology (JKUAT) and the National Council for Science, Technology and Innovation (NACOSTI) of Kenya for funding this research work. The JKUAT is acknowledged for providing testing laboratory services.

References

[1] J. Griesbach, Mango Growing in Kenya. ICRAF, Nairobi, Kenya, 2003
[2] H.Y. Nakasone and R.E. Paul, Crop Production Science in Horticulture, 1998.
[3] Ministry of Agriculture, Annual Report, 2007.
[4] Kenya Agriculture Research Institute (KARI), Annual Report, 1994.
[5] S. N. Jha, Development of a pilot scale evaporative cooled storage structure for fruits and vegetables for hot and dry region. Journal of Food Science and Technology, 2008. 45(2): 148-151.
[6] H. Uluko, C. L. Kanali, J. T. Mailutha, and D. Shitanda. A finite element model for the analysis of temperature and moisture distribution in a solar grain dryer. The Kenya Journal of Mechanical Engineering, 2006. 2(1): 47-56.
[7] F. W. Bakker-Arkema, J. De Baerdemaeker, P. Amirante, M. Ruiz-Altisent, and C. J. Studman. 1999. CIGR
[8] D. Shitanda, and N. V. Wanjala, Effects of different drying methods on the quality of Jute (Corchorus Olitorius L.). Drying Technology Journal, 2006. 24(1): 95-98.
[9] J.R. Camargo, C.D. Ebinuma, and J.L. Siveria, Experimental permormance of direct evaporative cooler operating during summer in Brazilian city. Int. J. of Refrigeration, 2005. 28(7), pp.1124-1132
[10] R. K. Kulkarni and S.P.S. Rajput, Comparative performance of evaporative cooling pads of alternative materials. (IJAEST) International journal of advanced engineering science and technology, 2011. Vol No.10, issue No. 2,239-244